



# An Experimental Study on Vibration-Driven Locomotion Systems Under Different Levels of Isotropic Friction

Ngoc-Tuan La<sup>1</sup>, Quoc-Huy Ngo<sup>2</sup>, Ky-Thanh Ho<sup>2</sup>,  
and Khac-Tuan Nguyen<sup>2</sup>✉

<sup>1</sup> Vinh University of Technology Education, Vinh, Vietnam

<sup>2</sup> Thai Nguyen University of Technology, Thai Nguyen, Vietnam  
tuannkn@tnut.edu.vn

**Abstract.** This paper shows experimental analysis results of the study on vibration-driven locomotion system, which can be applied in capsule robots. The experimental apparatus provided a capacity of varying friction force when keeping the weight of the whole system unchanged. Twelve experimental sets with 16 runs for each set were implemented, providing a deep insight of the system behavior, both in progression rate and the relative motions of the masses. The experimental data revealed that, the force ratio between the excitation magnitude and friction level would not be totally correct to present the excitation effects in modeling the system. The level of friction force may have a significant effect on not only how fast the system move, but also which direction of the progression. The new findings would be useful for further studies on the design and operation of vibration driven locomotion systems.

**Keywords:** Vibration-driven locomotion · Capsule robots · Isotropic friction

## 1 Introduction

Conventional mobile robots usually consist of external propulsion mechanisms, such as wheels, legs or paddles. Hence, such systems would face with several boundaries in terms of mechanical complexity, controllability, physical size, failure of moving parts, and causing hazard to surrounding environment. Recently, the development of mobile devices employing vibration for automotive motion has become a very promising solution for encapsulate locomotion systems [1–3]. The principle of this solution, pioneered by Chernousko [4], is that the forward and backward progression of the system can be obtained in the presence of dry friction combined with a periodically driven internal mass interacting with the main body of the system. An earlier model using vibro-impact driven mechanism was proposed by Pavlovskaja et al. [5]. On the one hand, the friction force is usually considered as a resistance preventing the moving trend of the system, and thus should not be too large. On the other hand, the presence of friction plays an important role of external resistance to provide the locomotion of the system in desired direction [1, 6]. The system working under small friction would not be able to progress in the desired direction.

Generally, the internal mass has been designed to have one of the two motion principles: 1) the mass moves periodically without having impact with the body and 2) the mass moves periodically and has impact (vibro-impact) with the body. In the former case, the relative motion of the internal mass must follow a specially designed multi-phase acceleration-controlled (see [7–10] for example). When the inertial force, caused by acceleration changes, exceeds the friction threshold, the body locomotion is generated. In many previous studies [1–10], the friction force was usually assumed to be isotropic, i.e. the friction forces in both forward and backward motion of the frame body have the same value. The latter choice of self-propelled design is vibration-impact driven locomotion. In this system, the internal mass oscillates and periodically collides with an obstacle block. This results in a jump-up of the inertial force, making the system move. The friction force was usually assumed to be isotropic [5, 11–16]. The system working under anisotropic friction, i.e. the friction in forward direction is different from that in backward direction, was also examined. However, the examined system requires a special control of the internal mass motion (See [17] for example) or can only move in the direction with smaller friction (downward of an inclined chute [18]).

The effectiveness of the robots has typically been considered by checking with the progression rate and dynamical response of the systems. In vibro-impact systems, the excitation force acting on the internal mass was usually in the sinusoidal form. In previous studies, the excitation force was treated as a dimensionless number, counted as the ratio between the real amplitude of the excitation force and the Coulomb friction value. The progression rate and/or moving direction of the system was checked as a function of such force ratio (See for example in [5, 12, 14–16]). In experimental studies, the effect of excitation force was taken into account with certain dry friction with given levels of frictional force (See [14, 19–22]). The effects of various friction levels on the system response have rarely been experimentally considered [3, 23] but not in interaction with the excitation force. Beside, some interesting observations have been reported [14, 24]. For example, when the elastic force acting on the capsule is larger than the threshold of the friction, backward motion of the capsule is observed [24]. At some situations, the average speed of forward progression of the capsule using small amplitude of excitation is much larger than the one with backward progression using large amplitude of excitation. This observation somehow reveals the fact that a large amplitude of excitation cannot improve the performance of the capsule system [14]. However, such interesting observations were found at certain conditions of experiments only and need more practical considerations and experimental validations. Consequently, this study was made to give deeper insights of the effect of different levels of friction force on the system response. Three levels of friction forces, representing for small, middle and large resistances were examined combined with four different values of the force ratios. The results revealed that with the same force ratio, the system have various behaviors with different levels of frictions. In addition, under the same friction force, varying the force ratio provides different trends of the moving direction of the vibration driven locomotion system.

The paper is organized as below. Basic principle of the vibration driven locomotion system is briefly presented in Sect. 2. The experimental setup is then described in detail

in Sect. 3. The results and discussions are given in Sect. 4. Some remarkable conclusions and recommendations are made in the last section.

## 2 Basic of the Study

### 2.1 Working Principle of the System

The physical model of a typical vibration-driven locomotion system with impacts is depicted in Fig. 1(a). The system is consisted of a body mass,  $m_2$  and an inertial mass,  $m_1$ . An elastic spring with stiffness  $k$  couples the two masses. The two masses are connected using an elastic spring and a viscous damper,  $c$ . The system body  $m_2$  can move along a straight line on a resistive horizontal plane. The internal mass oscillates inside the body along the line parallel to the motion line of the body. A harmonic force  $F_m$  with amplitude  $A$  and frequency  $\Omega$  exerts on both masses. The friction force,  $F_r$ , occurred at the contact surface between the body and the resistive plane is assumed to obey the Coulomb dry friction law, as shown in Fig. 1(b). In this study, the friction force is assumed to be isotropic, i.e.  $R^+ = |R^-| = R$ .

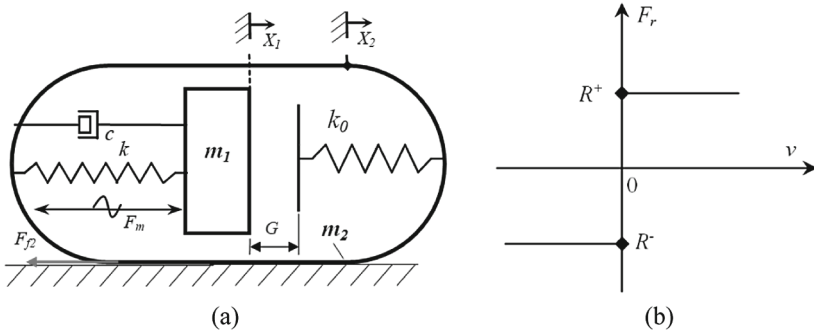


**Fig. 1.** A vibration-driven locomotion model (a) and Coulomb isotropic friction model (b)

Impact characteristics between the two masses were modeled as stiffness  $k_0$ . In Fig. 1,  $X_1$  and  $X_2$  represent the absolute displacements of the internal mass and the frame body, respectively. The motion  $X_i$  ( $i = 1, 2$ ) is considered as forward motion if the value of  $X_i$  is positive and vice versa.

The two masses are initially positioned with a gap  $G$ . When the relative displacement  $X_1 - X_2$  is greater than or equal to the gap  $G$ , impact occurs and the system can move forward.

The friction force plays a very important role in the working principle of the vibration locomotion systems [4, 5]. The system may either not progress or move in unexpected direction if the friction force is too small or too large. Naturally, in order to increase the average velocity of motion, the coefficient of friction of the body mass should be increased and that between the internal mass and the body mass decreased [4]. The results of this study would be a practical recommendation not only on the

upper limitation when increasing friction force but also the smallest friction, with respect to the excitation force, that can help the system move in desired direction.

### 2.2 Objectives of the Study

Generally, studies on the vibration-driven locomotion systems have usually been done by following steps:

- Describe the physical and mathematical models of the system;
- Implement experiments to validate the mathematical model;
- Analysis the system using the validated mathematical model, usually focus on the progression rate and the dynamical response of the system.

In order to expand the results to different scales of the prototypes, the mathematical model was usually transformed into dimensionless form.

The equations describing the motion of the system shown in Fig. 1 can be written as:

$$\begin{cases} m_1 \frac{d^2 X_1}{dt^2} = F_m - F_{spr} - c \left( \frac{dX_1}{dt} - \frac{dX_2}{dt} \right) - H [k_0(X_1 - X_2 - G)] \\ m_2 \frac{d^2 X_2}{dt^2} = -F_m + F_{spr} + c \left( \frac{dX_1}{dt} - \frac{dX_2}{dt} \right) + H [k_0(X_1 - X_2 - G)] - R \operatorname{sgn} \left( \frac{dX_2}{dt} \right) \\ F_m = A \cos(\Omega t) \end{cases} \quad (1)$$

where  $H$  is the Heaviside step function defined as:

$$H = \begin{cases} 1, & \text{if } (X_1 - X_2 - G) > 0 \\ 0, & \text{if } (X_1 - X_2 - G) \leq 0 \end{cases} \quad (2)$$

Assuming the spring is linear with the stiffness  $k$ , the spring force can be described as:

$$F_{spr} = k(X_1 - X_2) \quad (3)$$

Using the following non-dimensional variables and parameters:

$$\begin{aligned} \tau = \Omega_0 t; \quad x_1 = \frac{k}{R} X_1; \quad x_2 = \frac{k}{R} X_2; \quad \Omega_0 = \sqrt{\frac{k}{m_1}}; \quad \omega = \frac{\Omega}{\Omega_0}; \\ \zeta = \frac{c}{2m_1 \Omega_0}; \quad \alpha = \frac{A}{R}; \quad \sigma = \frac{k_0}{k}; \quad \gamma = \frac{k}{R} G; \quad \mu = \frac{m_2}{m_1} \end{aligned} \quad (4)$$

the dimensionless form of the model (1) can be expressed as:

$$\begin{cases} x_1'' = \alpha \cos(\omega \tau) - (x_1 - x_2) - 2\zeta(x_1' - x_2') - h\sigma(x_1 - x_2 - \gamma) \\ x_2'' = [-\alpha \cos(\omega \tau) + (x_1 - x_2) + 2\zeta(x_1' - x_2') + h\sigma(x_1 - x_2 - \gamma) - \operatorname{sgn}(x_2')] \frac{1}{\mu} \end{cases} \quad (5)$$

where  $()'$  and  $()''$  denotes the first and the second time derivative  $d()/d\tau$  and  $d^2()/d\tau^2$ , respectively; and  $h$  is a Heaviside function defined as:

$$h = \begin{cases} 1, & \text{if } (x_1 - x_2 - \gamma) > 0 \\ 0, & \text{if } (x_1 - x_2 - \gamma) \leq 0 \end{cases} \quad (6)$$

Generally, the effect of the excitation force ( $F_m$ ) on the system behavior have been taken into account by varying the value of the force ratio,  $\alpha$  (See [11, 13, 24, 25] for example). In the mentioned studies, a given value of  $\alpha$  provided one value of the dimensionless  $x_2$ . From Eq. (4), since both  $k$  and  $R$  are positive,  $x_2$  must have the same sign with  $X_2$ . It means that, for a given value of  $\alpha$ , different values of friction level  $R$  will result in different values of the progression  $X_2$ , but not different in the moving direction. Our experimental results revealed that with the same force ratio  $\alpha$ , the system can either move forward or backward, i.e. with different signs (either negative or positive) of the progression  $X_2$ . In other words, the force ratio,  $\alpha$  may not be totally correct to represent the effect of the excitation force, as usually suggested in many previous studies. Consequently, this study was made to experimentally examine of the effect of different levels of friction force on the system response. The results would provide a basic knowledge to give deeper insight into the locomotion systems working under different levels of the environmental resistance. Further work of modelling and analyzing the system can be made based on these findings.

The objectives of this study thus are as following:

- To develop an experimental apparatus which can vary the friction force when keeping the system weight;
- To carry out how different levels of the friction magnitude can effect on the progression rate of the system body under the same force ratio;
- To verify if the force ratio is not able to fully represent the excitation magnitude as previously suggested.

In this experimental study, three levels of friction forces, representing for small, middle and large resistances were examined combined with four different values of the force ratios. The experimental setup and implementing method are presented in the next section.

### 3 Experimental Implementation

The above model was realized as shown in Fig. 2, as developing from the apparatus built at TNUT's laboratory by Nguyen et al. [3, 13, 20].

A mini electro-dynamical shaker (1) is placed on a slider of a commercial linear bearing guide (4), providing a tiny rolling friction force. An additional mass (3) was clamped on the shaker shaft with the support of sheet springs (2). Generally, applying a sinusoidal current to the shaker leads to relative linear oscillation of the shaker shaft with the mass added on. Hereafter, the moveable mass, combined by the addition mass and the shaker shaft, is assigned as inertial mass,  $m_I$ , playing the role of the internal mass of the system. The relative motion of the inertial mass was measured by a non-contact position sensor (9). Motion of the shaker body was recognized by a linear variable displacement transformer (8). The body shaker, including the sensors and the

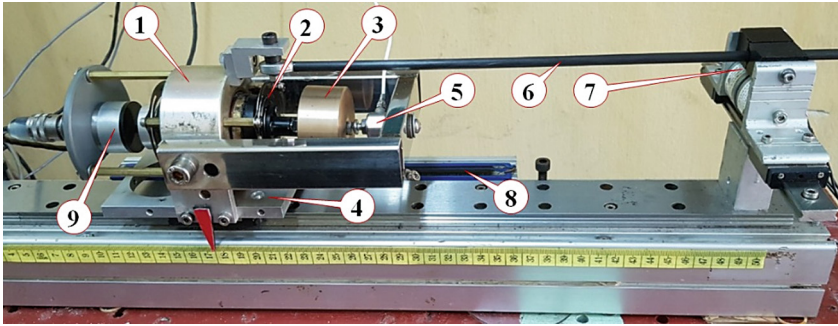


**Fig. 2.** A photograph of the experimental apparatus

carbon tube, is referred as the mass  $m_2$ . A force sensor (7) was used as the obstacle block to measure the impact force.

In order to vary the friction force when remaining the body mass, a carbon tube (5) is connected with the shaker body by means of a flexible joint, avoiding any misalignment when moving. The tube can slide between two aluminium pieces in the form of a V-block (6). The two V-blocks are fixed on two electromagnets, as depicted in Fig. 3(a). Supplying a certain value of electrical current to the coupled electromagnets provides a desired clamping force on the tube and thus a corresponding value of sliding friction. The friction force was measured by pulling the body to move at a steady speed. By adjusting the voltage supplied to the coupled electromagnets, the corresponding friction force can be obtained (See [3] for more detail).

The shaker is powered by a sinusoidal current generated by a laboratory function generator and then amplified by a commercial amplifier. The application of a sinusoidal current to the shaker leads to oscillation of the shaker shaft and the mass attached on it. As provided by the shaker supplier, the magnetic force,  $F_m$  is solely depended on the current supplied. Adjusting the sinusoidal supplying to the amplifier can provide a desired excitation force. A supplementary experiment was implemented to verify the relation of the magnetic force and the current supplied. A load cell was used as an obstacle resisting the shaker movement and thus to measure the magnetic force induced. A DC voltage was supplied to the shaker to generate the magnetic force. Varying the voltage, several pairs of the current passing the shaker and the force were collected. Experimental data confirmed that the excitation force is proportional to the current supplied to the shaker (see [13] for detailed information of how to determine this relation).

For operational parameters, three levels of friction force were selected at first. With respect to the total weight of the two masses as 2.336 kg, the friction force levels were set as 2.4, 6.8 and 13.6 N, corresponding to three levels of friction coefficient as approximately 0.1, 0.3 and 0.6. These levels can be respectively considered as low, middle and high friction coefficients. The minimum magnitude of the excitation force chosen needs to be strong enough to make the mass oscillate and collide to the obstacle block. Consequently, three higher levels of the excitation force were selected as strong

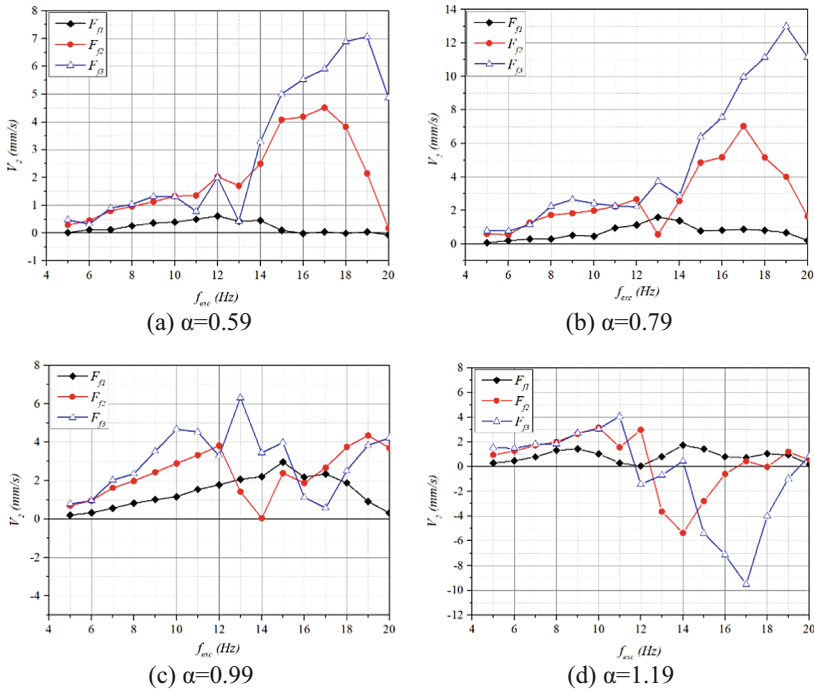


**Fig. 3.** Progression velocity of the system for (a)  $\alpha = 0.59$ ; (b)  $\alpha = 0.79$ ; (c)  $\alpha = 0.99$  and (d)  $\alpha = 1.19$ . For all sub-plots,  $F_{\beta} < F_{\gamma} < F_{\delta}$ .

enough to make significant differences between the system responses. The overall experimental parameters are given in Table 1.

**Table 1.** Parameters of experiments.

Parameter	Notation	Value	Unit
Internal mass	$m_1$	0.518	Kg
Body mass	$m_2$	1.818	Kg
Impact gap	$G$	0.5	mm
Friction force	$F_f$	2.4; 6.8; and 13.6	N
Force ratio	$\alpha = A/R$	0.59; 0.79; 0.99; and 1.19	–
Excitation frequency	$f_{exc}$	[5–20], 1 Hz step	Hz

Twelve sets of experiments were implemented for four levels of the force ratio,  $\alpha$  and three levels of the friction magnitude. Each experimental set, including 16 runs, was implemented at 16 values of the excitation frequency ranged from 5 Hz to 20 Hz with an incremental step of 1 Hz. Overall, excitation frequencies less than 5 Hz or higher than 20 Hz seemed as not efficient to operate the system. For each run, the data

of supply current passing the shaker, the displacements of the two masses and the impact force were collected and then analyzed. The results are shown in the next section.

### 4 Results and Discussion

Firstly, the progression rate of the whole system is considered. Figure 3 presents the average velocity of the system body at four levels of the force ratio,  $\alpha$ . As can be seen, for  $\alpha$  less than 1 (Fig. 3(a, b)), with the same  $\alpha$ , higher friction forces provided higher forward velocities. Increasing  $\alpha$  resulted in faster moving velocity of the forward motion of the system. However, forward velocities with  $\alpha \approx 1$  (Fig. 3c) provided a lower velocity, compared to that with  $\alpha = 0.79$ . The backward motion of the system appeared at then higher range of excitation frequency,  $f_{exc} = [12..18]$  Hz with the two highest levels of friction force ( $F_{f2}$  and  $F_{f3}$ ), as shown in Fig. 3d. From such observations, the following interesting issues can be remarked:

- It seems to be agreed with previous studies that, increasing the relative magnitude of the excitation with respects to friction force (i.e. increasing the force ratio  $\alpha$ ) may increase the forward velocity of the system;
- When the force ratio is higher than 1 (i.e. the excitation magnitude is larger than the friction force), backward motion would appear, even though the impact force is in forward direction;
- A new remarkable finding is that, with the same force ratio, the motion of the system would be either forward or backward, depending on the friction level. This would not agree with several previous suggestions that with a certain set of parameters, a given value of the force ratio provides only one direction of the system progression (As mentioned in the end of Sect. 2).

Another view of the effects of friction levels is depicted in Fig. 4 to support the above-mentioned ideas. At each of the two investigated levels of friction, the progression rate of the system with for levels of the force ratio are presented.

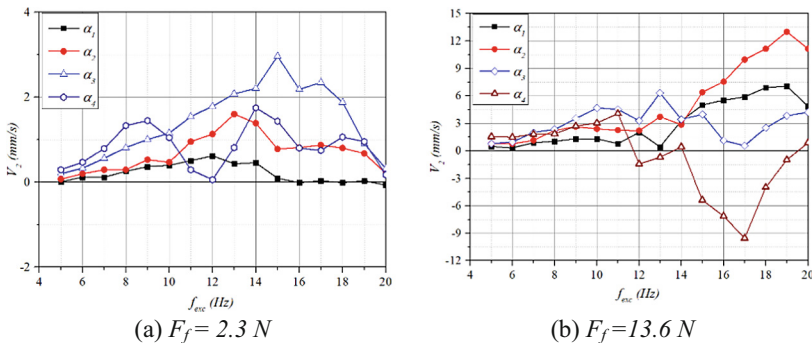


**Fig. 4.** Progression velocity of the system for (a)  $F_f = 2.3$  N; (b)  $F_f = 13.6$  N. For all sub-plots,  $\alpha_1 < \alpha_2 < \alpha_3 < \alpha_4$ .



As can be seen in Fig. 4, with the same friction level, higher force ratio would not provide higher progression rate. With low friction (Fig. 4a), the highest forward velocity was obtained at  $\alpha_3 = 0.99$ , whereas the highest force ratio ( $\alpha_4$ ) mostly provided lower velocity. With high level of the friction (Fig. 4b), highest forward velocity appeared with  $\alpha_2$ , whereas highest backward velocity performed at the highest level of force ratio,  $\alpha_4$ .

There has still been an open question about the reason of the backward motion of the system even though the impact force acting in the forward direction. Figure 5 illustrate the time history of the system motion. The two sub-plots have the same force ratio ( $\alpha = 1.19$ ) and other parameters, except that one for small friction (Fig. 5a,  $F_f = 2.3$  N) and one for large friction (Fig. 5b,  $F_f = 13.6$  N). Working with a small friction, the system appeared to move forward (Fig. 5a), whereas it moved backward with the larger friction (Fig. 5b). On each sub-plot, two red-thin vertical lines limit one oscillation period of the mass  $m_1$ . Another black-dash line divided each period into two areas: Area 1 where the body  $m_2$  moved forward, and area 2 where the body  $m_2$  moved backward.

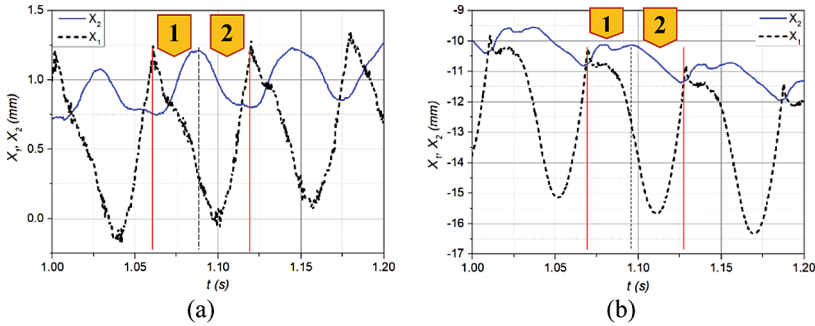


**Fig. 5.** Time histories of motions of the internal mass  $X_1$  (dash curve) and of the body  $X_2$  (blue solid curve): (a)  $F_f = 2.3$  N, and (b)  $F_f = 13.6$  N. A force ratio  $\alpha = 1.19$  was applied;  $f_{exc} = 17$  Hz.

As presented on the figure, the impacts occurred at the instant of the displacement peaks of  $m_1$ . Under small friction (Fig. 5a), the body moved forward not by impact, but for reaction between the two masses. The forward motion of the body occurred at somewhere when the mass  $m_1$  was going backward. Under higher friction (Fig. 5b), forward motion of the body seemed to be the result of impact force – it happened just at the impact instant. Different from that of the former case, in each period, the backward displacement was larger than the forward motion. Consequently, the overall motion of the system in this case was backward, although the impact already acted as a source for the forward moving of the system. Noted that negative values of the displacements,  $X_1$  and  $X_2$ , mean that the motions of the two masses were in backward direction, as relative to the origin coordinate ( $X_1 = X_2 = 0$ ).

From this practical observation, it can be concluded that forward motion of the system may not only depend on how large the impact force is, but also how the

interaction of the relative motion of the two masses. It is worth noting that, the mechanism behind of moving forward or backward motion of the whole system is till an open dynamic problem. The data obtained would be a good resource for further studies in the field.

## 5 Conclusions

This paper presented experimental observations and several initial analyses on a vibration driven locomotion apparatus. The experimental setup provided a capacity of varying friction force when keeping the weight of the whole system unchanged. Based on that, a series of experimental tests were implemented, providing a deep insight of the system behavior, both in progression rate and the relative motions of the masses. The following remarks would be useful for further studies:

- The force ratio between the excitation magnitude and friction level would not be totally correct to present the excitation effects in modeling the system;
- The level of friction force would be a significant effect on not only how fast the system move, but also which direction of the progression.

**Acknowledgement.** This research was funded by Vietnam Ministry of Education and Training, under the grant number B2019-TNA-04. The authors would like to express their thank to Thai Nguyen University of Technology, Thai Nguyen University, and Vinh University of Technology Education for their support for the study.

## References

1. Liu, P., Yu, H., Cang, S.: Modelling and analysis of dynamic frictional interactions of vibro-driven capsule systems with viscoelastic property. *Eur. J. Mech. A. Solids* **74**, 16–25 (2019)
2. Yan, Y., et al.: Proof-of-concept prototype development of the self-propelled capsule system for pipeline inspection. *Meccanica* **53**(8), 1997–2012 (2017)
3. Nguyen, V.-D., La, N.-T.: An improvement of vibration-driven locomotion module for capsule robots. *Mech. Based Des. Struct. Mach.* 1–15 (2020)
4. Chernous'ko, F.L.: The optimum rectilinear motion of a two-mass system. *J. Appl. Math. Mech.* **66**(1), 1–7 (2002)
5. Pavlovskaja, E., Wiercigroch, M., Grebogi, C.: Modeling of an impact system with a drift. *Phys. Rev. E: Stat. Nonlin. Soft Matter Phys.* **64**(5 Pt 2), 056224 (2001)
6. Chernous'ko, F.L.: Analysis and optimization of the motion of a body controlled by means of a movable internal mass. *J. Appl. Math. Mech.* **70**(6), 819–842 (2006)
7. Nunuparov, A., et al.: Dynamics and motion control of a capsule robot with an opposing spring. *Arch. Appl. Mech.* **89**(10), 2193–2208 (2019)
8. Huda, M.N., Yu, H.: Trajectory tracking control of an underactuated capsulobot. *Auton. Robots* **39**(2), 183–198 (2015)
9. Su, G., et al.: A design of the electromagnetic driver for the internal force-static friction capsulobot. In: 2009 IEEE/RSJ International Conference on Intelligent Robots and Systems (2009)

10. Li, H., Furuta, K., Chernousko, F.L.: Motion generation of the capsobot using internal force and static friction. In: Proceedings of the 45th IEEE Conference on Decision and Control (2006)
11. Gu, X.D., Deng, Z.C.H.: Dynamical analysis of vibro-impact capsule system with Hertzian contact model and random perturbation excitations. *Nonlinear Dyn.* **92**(4), 1781–1789 (2018). <https://doi.org/10.1007/s11071-018-4161-x>
12. Duong, T.-H., et al.: A new design for bidirectional autogenous mobile systems with two-side drifting impact oscillator. *Int. J. Mech. Sci.* **140**, 325–338 (2018)
13. Nguyen, V.-D., et al.: The effect of inertial mass and excitation frequency on a Duffing vibro-impact drifting system. *Int. J. Mech. Sci.* **124–125**, 9–21 (2017)
14. Liu, Y., Pavlovskaja, E., Wiercigroch, M.: Experimental verification of the vibro-impact capsule model. *Nonlinear Dyn.* **83**(1–2), 1029–1041 (2015)
15. Liu, P., et al.: A self-propelled robotic system with a visco-elastic joint: dynamics and motion analysis. *Eng. Comput.* **36**(2), 655–669 (2019)
16. Yan, Y., Liu, Y., Liao, M.: A comparative study of the vibro-impact capsule systems with one-sided and two-sided constraints. *Nonlinear Dyn.* **89**(2), 1063–1087 (2017)
17. Liu, P., Yu, H., Cang, S.: Optimized adaptive tracking control for an underactuated vibro-driven capsule system. *Nonlinear Dyn.* **94**(3), 1803–1817 (2018)
18. Xu, J., Fang, H.: Improving performance: recent progress on vibration-driven locomotion systems. *Nonlinear Dyn.* **98**(4), 2651–2669 (2019)
19. Nguyen, V.-D., et al.: A new design of horizontal electro-vibro-impact devices. *J. Comput. Nonlinear Dyn.* **12**(6), 061002 (2017)
20. Nguyen, V.-D., et al.: Identification of the effective control parameter to enhance the progression rate of vibro-impact devices with drift. *J. Vib. Acoust.* **140**(1), 011001 (2017)
21. Ho, J.-H., Nguyen, V.-D., Woo, K.-C.: Nonlinear dynamics of a new electro-vibro-impact system. *Nonlinear Dyn.* **63**(1–2), 35–49 (2010)
22. Su, G., et al.: A design of the electromagnetic driver for the “internal force-static friction” capsobot. In: The 2009 IEEE/RSJ International Conference on Intelligent Robots and Systems. IEEE (2009)
23. Nguyen, V.-D., Woo, K.-C., Pavlovskaja, E.: Experimental study and mathematical modelling of a new of vibro-impact moling device. *Int. J. Non-Linear Mech.* **43**(6), 542–550 (2008)
24. Liu, Y., et al.: Forward and backward motion control of a vibro-impact capsule system. *Int. J. Non-Linear Mech.* **70**, 30–46 (2015)
25. Liu, Y., et al.: Modelling of a vibro-impact capsule system. *Int. J. Mech. Sci.* **66**, 2–11 (2013)